Electron momentum distribution in cadmium sulfide

S. Perkkiö, S. Manninen, and T. Paakkari
Department of Physics, University of Helsinki, Siltavuorenpenger 20D, SF-00170 Helsinki 17, Finland
(Received 3 April 1989)

The isotropic and the directional electron momentum distributions in cadmium sulfide are studied by Compton scattering technique. The isotropic Compton profile has been measured from a polycrystalline CdS (wurtzite structure) sample and the directional profiles from the planes (0001) and $(10\bar{1}0)$ of single crystals, using 59.537-keV γ rays. The spherically averaged and directional ([0001], $[10\bar{1}0]$, and $[11\bar{2}0]$) Compton profiles have been calculated with use of linear combinations of atomic orbitals based on the symmetrical orthogonalization method. The experimental isotropic profile is found to be in quite good agreement with the theoretical one calculated with use of wave functions for free Cd^{2+} ion and S^{2-} ion in a spherical potential. The experimental and the calculated anisotropies are found to be in disagreement. The present calculational method is suitable for ionic solids, but our results for CdS reflect the need to take into account the partial covalent nature of the bonds between Cd and S.

I. INTRODUCTION

Compton scattering of x and γ rays has been successfully applied to determine the electron momentum distribution (EMD) of several materials.[1,2] This kind of study on wurtzite-structure materials is, however, infrequent and concerns mainly the average EMD. The anisotropy studies give valuable information about the bonding between the constituents of the material, and they are even more reliable than studies on a single profile, because the effects of several corrections to the measured data cancel out. So far, there are neither experimental nor theoretical EMD anisotropy studies on wurtzite-structure compounds comprised of group-II and -VI elements. The difficulties in growing single crystals large enough for Compton profile measurements have hindered the experiments. The theoretical determination of the electronic properties of wurtzite-structure compounds is complicated due to the low symmetry of the structure and the existence of four atoms in a unit cell. Moreover, the lattice constant ratio c/a deviates often slightly from the ideal value of 1.633.

The semiconducting cadmium compounds, especially the wurtzite polymorphs, are interesting because of their technical importance. Their physical properties have been studied widely, and quite recently, the electronic band structure of CdS in the wurtzite crystal structure was determined both experimentally and theoretically.[3–5] However, there have not been any attempts to use the band-structure data for determination of EMD's.

The Compton profile of wurtzite CdS in the crystal direction [0001] was measured by Jakimavičius and Purlys[6] using Mo $K\alpha$ radiation with an energy of 17.4 keV. They compared the experimental profile with some theoretical ones, but the agreement was found to be poor. Their experimental profile suffered from residual multiple-scattering effects and the evident failure of the impulse approximation. Therefore, it was decided to determine the average EMD and the EMD's in the main crystal directions [0001] and $[10\bar{1}0]$ of CdS by using a spectrometer based on ^{241}Am with γ-ray energy of 59.537 keV. Moreover, there was the possibility of calculating the corresponding Compton profiles in the LCAO (linear combination of atomic orbitals) approximation. The comparison of the experimental and theoretical profiles gives information about the validity of the LCAO approximation. It is most useful in the case of ionic solids, but the relative ionicity of CdS is only about 0.7.[7]

II. EXPERIMENTS

The experimental arrangement used in this study has been described in detail earlier.[8] γ rays with an energy of 59.537 keV emitted by an annular ^{241}Am source of activity of 5-Ci scatter from the sample in an evacuated chamber. The primary and scattered beams form an angle of 165° with each other (scattering angle), and angles of 75° and 90° with the sample surface, respectively. This corresponds to a Compton peak energy of 48.5 keV. An intrinsic Ge crystal (Princeton Gamma Technologies) cooled to liquid-nitrogen temperature (77 K) was used as a detector. A pile-up rejector was included in the system to prevent the summation of pulses. The channel width was about 63 eV or 0.1 a.u. of momentum and the total resolution of the Compton spectrometer was about 0.6 a.u. of momentum.

Cadmium sulfide single crystals in the wurtzite structure, delivered by Cleveland Crystals, Inc., were used to determine the Compton profile in the crystal directions [0001] and $[10\bar{1}0]$. The thickness of the crystals was 1.2 mm and the area perpendicular to the average scattering vector was 1.0 cm^2. The orientation of the single crystals was confirmed by x-ray diffraction. The isotropic Compton profile of CdS was measured by using a polycrystalline powder sample with a thickness of 1.15 mm. The purity of the powder (Fluka A.G. Buchs, Switzerland) was 99.999%.

The measuring time was about 3×10^5 s for the powder sample and 5×10^5 s for each of the single crystals. One photon in three seconds per channel was registered at the maximum of the profile.

Figure 1 shows the raw data for polycrystalline CdS accumulated during 3×10^5 s. The height of the elastic peak is about twice that of the Compton peak. The Ge $K\alpha$ escape peak at $p_z=1.8$ a.u. and a weaker Ge $K\beta$ escape peak cannot be seen because they are overlapped by the Compton profile. To minimize the effect of the escape peaks, the spectrum of the ^{241}Am calibration source was subtracted from the measured Compton spectra until the elastic component disappeared. To correct for the background, a no-sample measurement was made, and the scaled intensity was subtracted from the measured spectra. Then the low-energy tail was removed and the data were deconvoluted[9] to reduce the effect of the finite resolution of the detector. The data were also corrected for the energy dependence of the absorption and the relativistic cross section. The spectra were converted from energy to momentum scale and the profile was normalized to the area of the theoretical profile, 26.52 electrons, in the momentum range from 0.0 to 7.0 a.u. using intervals of 0.1 a.u. The 1s electrons of cadmium were neglected because they do not contribute to the experimental profiles at this momentum transfer. The contribution of double-scattering processes was estimated using two Monte Carlo methods.[10,11] The amount of double scattering was 4.5% of the total intensity and 1.8% and 2.0% at $J(0)$ for the powder and the single-crystal samples, respectively. Moreover, the amount of triple scattering was estimated by one of the Monte Carlo methods[11] and was found to be only 0.2% of the total intensity.

III. CALCULATIONS

The free-atom or -ion wave functions or wave functions for ions in different model potentials can be used for calculation of Compton profiles of solids in the LCAO approximation. The computing method used in this study

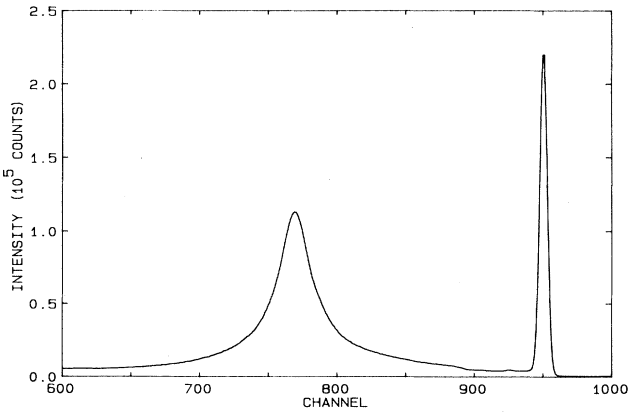

FIG. 1. Energy spectrum of 59.537-keV γ rays scattered through a mean angle of 165° from a polycrystalline CdS sample. The channel width is about 63 eV.

was developed by Aikala initially for primitive crystals[12,13] (representable as Bravais lattices) and later extended to nonprimitive crystals (representable as Bravais lattices with a basis).[14] As the wave functions ψ are nonorthogonal, when they are localized to different lattice sites (μ,ν), overlap integrals of the form

$$\Delta_{\mu\nu}=\int\psi_\mu^*(\mathbf{r})\psi_\nu(\mathbf{r})d\mathbf{r} \tag{1}$$

exist. The initially nonorthogonal functions are orthonormalized by using Löwdin's symmetrical method.[15] The first-order density matrix for one crystal atom g is then defined as[12]

$$\rho_g(\mathbf{r},\mathbf{r}')=2\sum_{\mu\in g}\sum_\nu\psi_\mu(\mathbf{r})(\Delta^{-1})_{\mu\nu}\psi_\nu^*(\mathbf{r}')\ , \tag{2}$$

and $(\Delta^{-1})_{\mu\nu}$ is the inverse overlap matrix element between the states ψ_μ and ψ_ν localized in different atoms of the crystal. The corresponding momentum density $\rho_g(\mathbf{p})$ is obtained by a double Fourier transform as

$$\rho_g(\mathbf{p})=2\sum_\mu\sum_\nu\chi_\mu(\mathbf{p})(\Delta^{-1})_{\mu\nu}\chi_\nu^*(\mathbf{p})\ , \tag{3}$$

where $\chi(\mathbf{p})$ is the electron wave function in momentum space, given by the Fourier transform of the real-space wave function $\psi(\mathbf{r})$,

$$\chi(\mathbf{p})=(2\pi)^{-3/2}\int\psi(\mathbf{r})e^{i\mathbf{p}\cdot\mathbf{r}}d\mathbf{r}\ . \tag{4}$$

The Compton profile is the one-dimensional projection of $\rho(\mathbf{p})$ in the desired direction,[1]

$$J(p_z)=\int_{-\infty}^{\infty}\int_{-\infty}^{\infty}\rho(\mathbf{p})dp_x\,dp_y\ . \tag{5}$$

The details for computing the Compton profiles from the first-order density matrix are given in Refs. 12–14.

To calculate the inverse overlap matrix Δ^{-1} the Fourier-series method[16] is employed. The metric matrix (the overlap matrix) Δ is first partly diagonalized by a unitary transformation and the small diagonal blocks are inverted. Thereafter, the inverse Fourier transform is calculated, and this gives the inverse metric matrix elements. We have extended this method to the C_{3v}-symmetry point group of the wurtzite structure along the lines presented for the site-symmetry point groups D_{2h}, D_{6h}, and O_h by Aikala.[16]

The computer programs were rewritten in standard FORTRAN 77 language and installed on a Digital Equipment Corporation VAX 8650 computer. The programs were checked by reproducing the spherically averaged and the directional Compton profiles for NaF.[17]

Wave functions for neutral free Cd and S atoms,[18] Cd^+ and S^- ions,[18] and Cd^{2+} and S^{2-} ions,[18–20] where the sulfide ion was supposed to be free or in spherical potentials of various radii, were used to calculate the Compton profiles. The ground-state electron configuration is core$+4d^{10}5s^2$ and core$+3s^23p^4$ for Cd and S, respectively. The overlap effects were calculated for the 4d and 5s states of Cd and for the 3s and 3p states of S. This makes 20 states altogether in the case of CdS and Cd^+S^- and 18 states in the case of $Cd^{2+}S^{2-}$. Twenty-one nearest orders of neighbors were included in the orthogonalization and in the calculation of the corrections to the Compton

profiles. Lattice parameters were taken as $a=4.1348$ Å and $c=6.7490$ Å.[21] The overlap effects for the Cd^{2+} and S^{2-} (in a spherical potential) ions only were found to be small enough for the Fourier-series method to give reliable results.[16] The maximum overlap was about 0.08 for these ions and about 0.3 for the other cases. Moreover, the convergence of the Compton profiles, which was checked by using various numbers of neighbor orders and integration points in the numerical integrations, was achieved only by using these wave functions. Therefore, only the results for the case $Cd^{2+}S^{2-}$ will be considered in the following.

IV. RESULTS AND DISCUSSION

The experimental isotropic and directional Compton profiles for CdS after all corrections are given in Table I. The experimental profile $J_{[0001]}$ has a lower electron momentum density at low momenta than the isotropic experimental profile, which in turn has a lower electron momentum density at low momenta than the profile $J_{[10\bar{1}0]}$. Thus, for $p_z=0$ a.u. the Compton profile is higher in the nonbonding $[10\bar{1}0]$ direction than in the bonding [0001] direction.

The $J(0)$ values for the free-ion and the isotropic LCAO profiles are given in Table II for different wave-function combinations of Cd^{2+} and S^{2-} ions. Moreover, the quantity

$$\Delta^2=\sum_{0.0\le p_z\le 7.0\text{ a.u.}}|J_{\text{theor}}(p_z)-J_{\text{expt}}(p_z)|^2\ ,$$

which gives information about the overall agreement of the theoretical and experimental Compton profiles, has been calculated using theoretical LCAO profiles convoluted with the residual instrument function (RIF) of the experiment (cf. Table III, last column). The wave-function combinations 5 and 6 are found to be best in describing the experimental isotropic profile in the whole p_z range.

The crystal Compton profiles in the LCAO approximation for the $Cd^{2+}S^{2-}$ configuration calculated by using wave-function combination 5 [a free Cd^{2+} ion[20] and a S^{2-} ion in a spherical potential of radius 3.477 a.u. (Ref. 19)] are given in Table III. In addition to the spherically averaged and the various directional profiles, the free-ion Compton profile is included.

The difference between the experimental isotropic profile and the spherically averaged LCAO profile convoluted with the residual instrument function of the experiment is plotted in Fig. 2 for wave-function combinations 2, 5, and 6. Moreover, the corresponding difference for the free-ion profile calculated from wave-function combination 5 and for the free-atom profile from Ref. 22 are plotted. One can clearly see that the free-ion profile is a much better approximation than the free-atom profile, and the overlap correction brings the theory closer to the experimental values near the peak of the profile. It can be mentioned that the radius 3.477 a.u. is given by Pauling[23] for the S^{2-} ion and it is seen to give the best agreement with the experiment near $p_z=0$ a.u.

The impulse approximation seems to be valid for other

TABLE I. Experimental isotropic and directional Compton profiles for CdS. The statistical error σ is given at some p_z values.

p_z (a.u.)	$J_{(\text{isotropic})}$	σ	$J_{[0001]}$	$J_{[10\bar{1}0]}$	σ
0.0	12.399	±0.020	12.347	12.437	±0.014
0.1	12.318		12.268	12.346	
0.2	12.098		12.060	12.120	
0.3	11.751		11.731	11.778	
0.4	11.295		11.303	11.325	
0.5	10.758		10.793	10.788	
0.6	10.169		10.224	10.196	
0.7	9.553		9.624	9.576	
0.8	8.939		9.016	8.953	
0.9	8.346		8.419	8.353	
1.0	7.792	±0.016	7.852	7.791	±0.011
1.2	6.844		6.857	6.836	
1.4	6.107		6.067	6.087	
1.6	5.505		5.447	5.479	
1.8	4.967		4.938	4.951	
2.0	4.474	±0.012	4.492	4.476	±0.008
2.5	3.489		3.532	3.507	
3.0	2.803		2.803	2.808	
3.5	2.329		2.311	2.320	
4.0	1.992	±0.008	1.978	1.979	±0.005
5.0	1.526		1.520	1.526	
6.0	1.218		1.209	1.212	
7.0	0.963	±0.005	0.954	0.956	±0.003

than K electrons of Cd. According to the binding-energy criterion, the impulse approximation is valid when the recoil energy (RE) is larger than about twice the binding energy[24] (BE) and the square of the BE-to-RE ratio gives the accuracy of the approximation.[25] The binding energies for L electrons of Cd are 4.018, 3.727, and 3.538 keV (Ref. 26) and the recoil energy varies from about 11 to 7 keV at p_z values from 0 to 7 a.u. in this experimental arrangement. Thus the binding-energy criterion is fulfilled at least in the p_z range from 0 to 5 a.u. corresponding to the recoil energy from 11 to 8 keV. The confidence of the impulse approximation varies from 10% to 25% for the L electrons of Cd. In the case of palladium, the Compton profile measured by 60-keV photons was found to be in excellent agreement with the results obtained by 320-keV photons.[27,28] The L-shell binding energies for Cd are not very different from those of Pd and thus one can conclude that the impulse approximation is valid for L electrons of Cd.

The theoretical anisotropies $\Delta J_1 = J_{[0001]} - J_{[10\bar{1}0]}$, $\Delta J_2 = J_{[0001]} - J_{[11\bar{2}0]}$, and $\Delta J_3 = J_{[10\bar{1}0]} - J_{[11\bar{2}0]}$ calculated for wave-function combination 5 are plotted in Fig. 3. They have not been convoluted by the residual instrument function of the experiment. The ΔJ_1 and ΔJ_2 curves closely resemble each other, the anisotropy being slightly larger for ΔJ_1 near the peak of the profiles. At the the peak of the profiles the anisotropies ΔJ_1 and ΔJ_2 are 1.4% and 1.1% of the $J(0)$ value, respectively, but ΔJ_3 is only 0.2% of the $J(0)$ value. This is understandable on the basis of the wurtzite structure, where the planes $(10\bar{1}0)$ and $(11\bar{2}0)$ are directed about equally in contrast to the (0001) planes.

TABLE II. $J(0)$ values for the free-ion and the isotropic LCAO Compton profiles calculated using different wave-function combinations (wf) for Cd^{2+} and S^{2-}: For 1, 2, and 3 Cd^{2+} from Clementi and Roetti (Ref. 18) excluding the 5s contribution and S^{2-} of various radii from Paschalis and Weiss (Ref. 19); for 4, 5, and 6 Cd^{2+} from Richardson *et al.* (Ref. 20) and S^{2-} from Paschalis and Weiss (Ref. 19). The quantity $\Delta^2 = \sum_{0.0 \le p_z \le 7.0 \text{ a.u.}} |J_{\text{theor}}(p_z) - J_{\text{expt}}(p_z)|^2$.

wf	S^{2-} radius (a.u.)	Free	LCAO	Δ^2
1	3.137	12.526	12.388	0.31
2	3.477	12.720	12.555	0.27
3	3.817	12.894	12.705	0.39
4	3.137	12.370	12.247	0.45
5	3.477	12.564	12.414	0.22
6	3.817	12.738	12.564	0.18

The experimental anisotropy $J_{[0001]} - J_{[10\bar{1}0]}$ is given in Fig. 4 together with the theoretical ones calculated for different S^{2-}-ion radii and convoluted with the residual instrument function of the experiment. One can clearly see that the experimental and the theoretical anisotropies are not consistent with each other. The details of the theoretical curves after the second maximum are smeared off in the convolution process with the residual instru-

TABLE III. Spherically averaged and directional ([0001], $[10\bar{1}0]$, $[11\bar{2}0]$) LCAO and the free-ion Compton profiles for $Cd^{2+}S^{2-}$ calculated from wave-function combination 5 (Table II). The residual instrument function (RIF) of the present experiments is also given. The profiles are not convoluted with the RIF of the experiment.

p_z (a.u.)	$J_{(av)}$	$J_{[0001]}$	$J_{[10\bar{1}0]}$	$J_{[11\bar{2}0]}$	$J_{(free)}$	RIF
0.0	12.414	12.517	12.344	12.374	12.564	1.600
0.1	12.355	12.458	12.280	12.304	12.497	1.522
0.2	12.154	12.220	12.095	12.097	12.274	1.305
0.3	11.798	11.775	11.788	11.760	11.872	0.992
0.4	11.313	11.225	11.351	11.308	11.323	0.642
0.5	10.744	10.667	10.806	10.786	10.697	0.316
0.6	10.140	10.104	10.200	10.224	10.056	0.056
0.7	9.532	9.520	9.572	9.618	9.436	−0.114
0.8	8.939	8.938	8.951	8.979	8.856	−0.193
0.9	8.377	8.389	8.367	8.363	8.321	−0.198
1.0	7.863	7.882	7.846	7.823	7.832	−0.155
1.2	7.005	7.000	7.002	6.985	6.978	−0.031
1.4	6.299	6.288	6.302	6.310	6.254	0.041
1.6	5.664	5.665	5.665	5.674	5.623	0.041
1.8	5.083	5.090	5.083	5.082	5.060	0.012
2.0	4.563	4.568	4.564	4.561	4.552	−0.008
2.5	3.520	3.515	3.520	3.519	3.514	−0.001
3.0	2.790	2.790	2.790	2.792	2.786	0.001
3.5	2.296	2.299	2.297	2.294	2.293	0.0
4.0	1.951	1.949	1.951	1.952	1.950	0.0
5.0	1.486	1.487	1.486	1.486	1.485	0.0
6.0	1.159	1.159	1.159	1.158	1.158	0.0
7.0	0.908	0.908	0.908	0.907	0.907	0.0

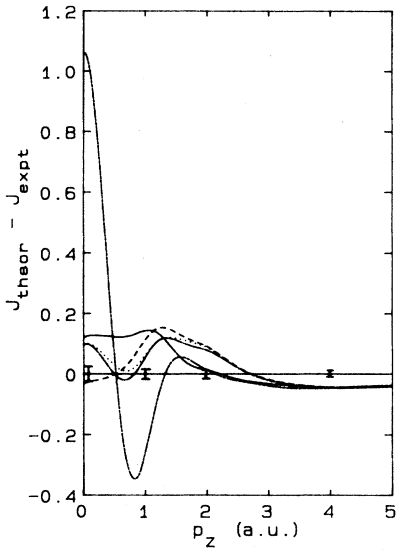

FIG. 2. Comparison of the experimental and the theoretical isotropic Compton profiles for CdS. The difference between the spherically averaged LCAO profile convoluted with the residual instrument function of the experiment and the experimental isotropic profile for different wave functions: the Cd^{2+} ion from Ref. 17 combined with the S^{2-} ion of radius 3.477 a.u. from Ref. 18 (solid curve), the Cd^{2+} ion from Ref. 19 combined with the S^{2-} ion of radius 3.477 a.u. (dashed curve) and 3.817 a.u. (dotted curve) from Ref. 18. The difference corresponding the dashed curve without orthogonalization corrections (dot-dashed curve) and the free-atom (double dot-dashed curve) profile is also given. Error bars (σ) are shown at selected p_z values.

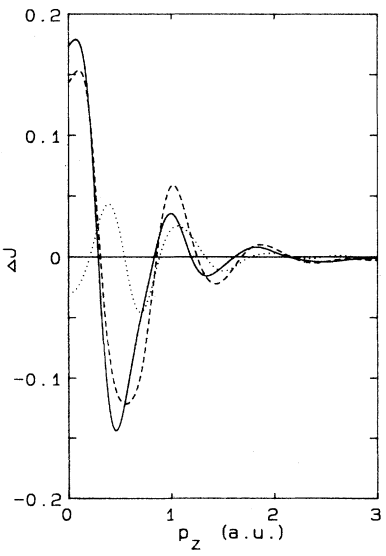

FIG. 3. Difference ΔJ between the directional Compton profiles of CdS in the LCAO approximation: $J_{[0001]} - J_{[10\bar{1}0]}$ (solid curve), $J_{[0001]} - J_{[11\bar{2}0]}$ (dashed curve), and $J_{[10\bar{1}0]} - J_{[11\bar{2}0]}$ (dotted curve). Wave functions for the Cd^{2+} ion were from Ref. 19 and for the S^{2-} ion (radius 3.477 a.u.) from Ref. 18.

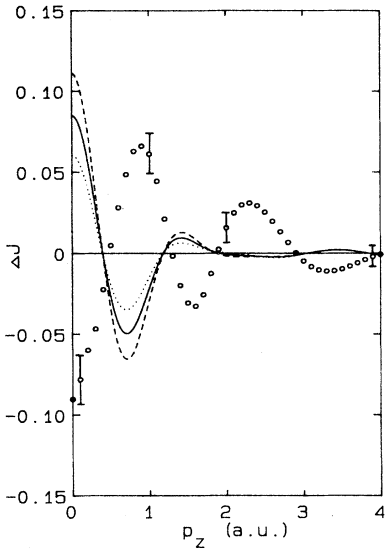

FIG. 4. Comparison of the experimental and the theoretical anisotropy $\Delta J = J_{[0001]} - J_{[10\bar{1}0]}$. The experimental result is given by circles and error bars (σ) are shown at selected p_z values. The theoretical curves are convoluted with the residual instrument function of the experiment and correspond to the S^{2-}-ion radii 3.817 a.u. (dashed curve), 3.477 a.u. (solid curve), and 3.137 a.u. (dotted curve).

ment function. For fair comparison, the theoretical anisotropies should include also the effect of the annular source geometry of the experiment (the direction of the scattering vector is not constant). In the case of MgO the effect of this was to reduce the minima and the maxima by about 14% when the scattering angle was 166°.[29] However, this cannot be applied directly to the present case because now the structure is hexagonal; the method developed by Aikala[29] deals only with cubic structures.

The anisotropy is not sensitive to the S^{2-}-ion representation. The same conclusion can be made also in the case of MgO about the O^{2-}-ion representation.[30] Therefore, the reason for the inconsistency of the anisotropies evidently lies in the model used for the calculation. The wave functions used here for Cd^{2+} and S^{2-} can be taken as representatives and the basic features of the anisotropies can be supposed to remain the same when the potential for the S^{2-} ion is changed.

As mentioned earlier, the fractional ionic character of CdS is 0.7 and thus the bonds have a significant amount of covalent nature. The ionic description $Cd^{2+}S^{2-}$ is not then completely justified, although it interprets the isotropic Compton profile fairly well. Instead, some hybridization to sp^3 orbitals occurs. The interstitial electronic distribution is localized in preferred directions, which affects the anisotropy in momentum space also. The calculations reported here are based on complete ionic description with no preferred directions in the electron density.

The quantitative comparison of the present data with the results given by Jakimavičius and Purlys[6] is impossible because no numerical results were given. They tried

to interpret the Compton profile of CdS using different theoretical approximations with little success. Wave functions for ions Cd^{2+} and S^{2-} were not used.

In many cases the structure of the material determines the basic features of the anisotropy of the Compton profile. This was predicted, e.g., for tetrahedrally bonded semiconductors of the zinc sulfide type.[31] Although there are only few studies concerning wurtzite-structure materials, anisotropy studies on hexagonal boron nitride[32] are worth mentioning. The anisotropy $J_{[0001]} - J_{[\perp(0001)]}$ measured from pyrolytic samples and the anisotropy calculated in the LCAO approximation disagreed, especially at low momenta. This anisotropy was found to be slightly negative experimentally and slightly positive in the LCAO approximation close to $p_z = 0.0$ a.u. Better agreement of the experimental and the theoretical anisotropies was found with the molecular-orbital calculation and the pseudopotential calculation. Thus, the same type of discrepancy between the experimental and the LCAO anisotropies is observed in BN and in the present case of CdS. However, no direct conclusions can be made from these two cases only because the materials are of different nature. Also, the details of the computations differ.

V. CONCLUSIONS

Compton profiles of CdS have been measured with high statistical accuracy. The isotropic Compton profile of CdS is fairly accurately reproduced in the calculation process based on the LCAO approximation when using the wave functions for the free Cd^{2+} ion and the S^{2-} ion in a spherical potential. However, the LCAO model fails to interpret the experimental anisotropies. The free-atom or -ion wave functions for sulfur are found unsuitable, but instead the sulfide ion has to be placed in a potential describing the crystal surroundings. Calculations of Compton profiles for wurtzite materials using other models are suggested. The determination of Compton profiles for other compounds having the wurtzite structure is in progress in order to examine their common features.

ACKNOWLEDGMENTS

Dr. Oiva Aikala is gratefully acknowledged for providing the authors with the computer programs for calculation of the LCAO Compton profiles.

[1] *Compton Scattering,* edited by B. G. Williams (McGraw-Hill, New York, 1977).
[2] M. J. Cooper, Rep. Prog. Phys. **48**, 415 (1985).
[3] K. J. Chang, S. Froyen, and M. L. Cohen, Phys. Rev. B **28**, 4736 (1983).
[4] N. G. Stoffel, Phys. Rev. B **28**, 3306 (1983).
[5] K. O. Magnusson and S. A. Flodström, Phys. Rev. B **38**, 1285 (1988).
[6] J. A. Jakimavičius and R. P. Purlys, Phys. Status Solidi B **131**, K63 (1985).
[7] J. C. Phillips and J. A. Van Vechten, Phys. Rev. Lett. **22**, 705 (1969).
[8] S. Manninen and T. Paakkari, Nucl. Instrum. Methods **155**, 115 (1978).
[9] R. Serimaa, O. Serimaa, P. Paatero, and T. Paakkari, University of Helsinki Report No. HU-P-232, 1984 (unpublished).
[10] V. Halonen, B. Williams, and T. Paakkari, Phys. Fenn. **10**, 107 (1975).
[11] J. Felsteiner, P. Pattison, and M. J. Cooper, Philos. Mag. **30**, 537 (1974).
[12] O. Aikala, Philos. Mag. **31**, 935 (1975).
[13] O. Aikala, Philos. Mag. **32**, 333 (1975).
[14] O. Aikala, Philos. Mag. **33**, 603 (1976).
[15] P. O. Löwdin, Adv. Phys. **5**, 1 (1956).
[16] O. Aikala, J. Phys. C **16**, 2217 (1983).
[17] J. Redinger, R. Podloucky, S. Manninen, T. Pitkänen, and O. Aikala, Acta Crystallogr. Sect. A **45**, 478 (1989).
[18] E. Clementi and C. Roetti, At. Data Nucl. Data Tables **14**, 177 (1974).
[19] E. Paschalis and A. Weiss, Theor. Chim. Acta **13**, 381 (1969).
[20] J. W. Richardson, M. J. Blackman, and J. E. Ranochak, J. Chem. Phys. **58**, 3010 (1973).
[21] R. W. G. Wyckoff, *Crystal Structures,* 2nd ed. (Wiley, New York, 1963), Vol. 1.
[22] F. Biggs, L. B. Mendelsohn, and J. B. Mann, At. Data Nucl. Data Tables **16**, 201 (1975).
[23] L. Pauling, *The Nature of the Chemical Bond,* 3rd ed. (Cornell University Press, Ithaca, NY, 1967).
[24] B. J. Bloch and L. B. Mendelsohn, Phys. Rev. A **9**, 129 (1974).
[25] P. Eisenberger and P. M. Platzman, Phys. Rev. A **2**, 415 (1970).
[26] J. A. Bearden and A. F. Burr, Rev. Mod. Phys. **39**, 125 (1967).
[27] A. Gupta, B. K. Sharma, H. Singh, and S. Perkkiö, in *Current Trends in the Physics of Materials,* edited by M. Yussouff (World Scientific, Singapore, 1987), pp. 156–160.
[28] B. K. Sharma, A. Gupta, H. Singh, S. Perkkiö, A. Kshirsagar, and D. G. Kanhere, Phys. Rev. B **37**, 6821 (1988).
[29] O. Aikala, Phys. Status Solidi B **110**, K107 (1982).
[30] O. Aikala, T. Paakkari, and S. Manninen, Acta Crystallogr. Sect. A **38**, 155 (1982).
[31] H. Nara, T. Kobayasi, and K. Shindo, J. Phys. C **17**, 3967 (1984).
[32] R. Tyk, J. Felsteiner, I. Gertner, and R. Moreh, Phys. Rev. B **32**, 2625 (1985).